

to perform an experimental study of the melilite system with the introduction of increasing amounts of fluorine.

References

- AHMED, F. R. & CRUICKSHANK, D. W. J. (1953). *Acta Cryst.* **6**, 385.
 BOOTH, A. D. (1946). *Proc. Roy. Soc. A*, **188**, 77.
 BRÖGGER, W. C. (1890). *Z. Kristallogr.* **16**, 279.
 CANNILLO, E., GIUSEPPE, G. & TAZZOLI, V. (1967). *Acta Cryst.* **23**, 255.
 DARLOW, S. F. (1960). *Acta Cryst.* **13**, 683.
 GORIA, C. (1953). *Atti Accad. Torino, Classe sci. fis. mat. nat.* **88**, 153.
 MOORE, F. H. (1963). *Acta Cryst.* **16**, 1169.
 PENG, C.-S., TSAO, Y.-L. & CHOU, T.-Y. (1962). *Scientia Sinica*, **11**, 977.
 SGARLATA, F. (1965). *Period. Min.* **34**, 401.
 SMITH, J. V. (1953). *Amer. Min.* **38**, 643.
 ZACHARIASEN, W. H. (1930). *Z. Kristallogr.* **74**, 226.
 ZACHARIASEN, W. H. (1931). *Norsk geol. Tidsskr.* **12**, 577.
 ZOLTAI, T. (1960). *Amer. Min.* **45**, 960.

Acta Cryst. (1967). **23**, 264

The Crystal Structure of Pb_3UO_6

BY META STERNS

Department of Chemistry, School of General Studies, Australian National University, Canberra, Australia

(Received 25 October 1966)

The structure of Pb_3UO_6 has been determined from single-crystal data, by analysis of the three-dimensional Patterson distribution, Fourier and $\Delta\rho$ syntheses and subsequent block-diagonal least-squares refinement to a final R value of 0.068. The unit cell is orthorhombic, space group $Pnam$, with $a = 13.71$, $b = 12.36$, $c = 8.21$ Å and $Z = 8$. The uranium atoms are octahedrally coordinated to six oxygen atoms and the slightly distorted octahedra, by sharing apices, form infinite staggered chains in the z direction, the lead atoms and the remaining oxygen atoms being distributed in a rather irregular array between the chains.

Introduction

In the course of a systematic study of mixed oxides of uranium(VI) and lead(II), four discrete compounds, Pb_3UO_6 , $\text{Pb}_{11}\text{U}_5\text{O}_{26}$, PbUO_4 and $\text{Pb}_5\text{U}_{19}\text{O}_{62}$ were prepared by solid-state reactions of oxide mixtures and characterized by chemical and X-ray powder phase analysis. Of these, only the monouranate PbUO_4 has been described in the literature (Fron del & Barnes, 1958; Kovba, Polunina, Simanov & Ippolitova, 1961) and the conclusion of Fron del & Barnes that it is isostructural with BaUO_4 , the structure of which has been determined by Samson & Sillén (1947), was confirmed by means of X-ray powder data. The new uranate Pb_3UO_6 could have been expected to be similar in structure to the known uranates Ba_3UO_6 , Sr_3UO_6 and Ca_3UO_6 , all of which have the same distorted cryolite type structure (Rüdorff & Pfitzer, 1954; Sleight & Ward, 1962; Rietveld, 1966) but a preliminary X-ray investigation of the polycrystalline material indicated a completely different type of structure, previously not encountered in any uranate. Therefore, when single-crystal fragments were isolated from preparations of this phase, a complete structure determination was undertaken, the results of which are described here. A general survey of the system Pb-U-O and X-ray work on the other lead uranates will be published separately.

Experimental

Single-phase material Pb_3UO_6 was prepared in polycrystalline form by heating pelleted stoichiometric mixtures of PbUO_4 (or U_3O_8) and PbO at 600–650°C. Heating at higher temperatures, to achieve sintering and possibly an increase in the crystallite size, resulted in decomposition of Pb_3UO_6 to $\text{Pb}_{11}\text{U}_5\text{O}_{26}$ and PbO . Only by heating Pb_3UO_6 in an excess of PbO ($\text{Pb:U} \sim 20:1$) at 800°C could sintered dark red Pb_3UO_6 be obtained, in a matrix of pale yellow PbO . The latter could not be leached out selectively, since any solvent for PbO also dissolves the uranate. The two phases had therefore to be separated by hand-picking the crushed mass under the microscope, and after careful examination for phase purity fragments suitable for single-crystal work were selected. The crystal fragments were usually lath-shaped, with no morphological faces, the longest dimension being mainly along the c axis and the shortest along the b axis.

Unit-cell dimensions were determined from oscillation and Weissenberg photographs and also from Guinier powder patterns of the polycrystalline material, calibrated internally with potassium chloride. The unit cell is orthorhombic;

$$a = 13.71 \pm 0.01, \quad b = 12.36 \pm 0.01, \quad c = 8.21 \pm 0.005 \text{ \AA}, \\ U = 1391 \text{ \AA}^3, \text{ F.W. } 955.6.$$

With the pycnometrically determined $D_m = 9.01 \text{ g.cm}^{-3}$, $Z = 8$.

Owing to the very irregular shape of the crystal fragments, reliable absorption corrections could not be applied and attempts to shape the crystals by grinding failed because of cleavage across the b axis. It was therefore sought to minimize absorption errors by the use of very small crystal fragments, aiming at an overall value of $\mu r \sim 1$. Approximate dimensions of the selected crystals were $0.02 \times 0.015 \times 0.08 \text{ mm}$ for Mo $K\alpha$ radiation ($\mu_{\text{Mo}} = 990 \text{ cm}^{-1}$) and $0.02 \times 0.01 \times 0.05 \text{ mm}$ for Cu $K\alpha$ radiation ($\mu_{\text{Cu}} = 2082 \text{ cm}^{-1}$).

Data for six layers around the c axis (hkL with $L = 0$ to 5) were collected from multiple film equi-inclination Weissenberg photographs using initially Mo $K\alpha$ radiation. Intensities were estimated visually against a scale of timed exposures of a reflexion from the same crystal, averaging over equivalent reflexions and correcting for spot area. With exposure times of the order of 200 hours for each layer, about 700 independent reflexions could be recorded, representing, because of the small size of the crystal, only *ca.* 50% of the possible number.

In order to detect weak reflexions not recorded in this set, avoiding prohibitive exposure times, a corresponding set of six-layer data was recorded with Cu $K\alpha$ radiation, using the rotating anode high-power X-ray generator (200 mA, 30 kV) at the C.S.I.R.O. Division of Chemical Physics, Melbourne. This second set of data, with average exposures of 20 hours, gave about 200 additional reflexions and also allowed the systematic absences to be established definitively.

After interlayer scaling of both sets of derived F^2 values (using $h0l$ data) and their correlation, the values were brought to an approximately absolute scale by means of a Wilson plot. Owing to scatter of the experimental points, no reliable value of the temperature factor could be deduced from the plot at this stage.

A total of 814 out of 1212 possible terms in the Cu radiation sphere were used in the subsequent analysis, the small number of reflexions outside this sphere being omitted.

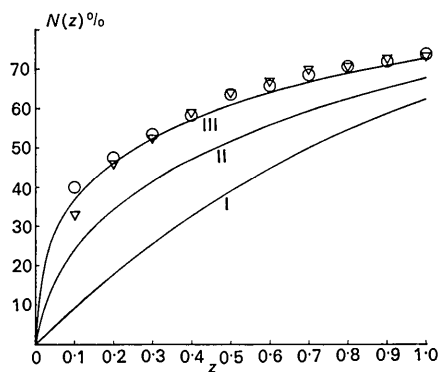


Fig. 1. Comparison of the experimental distribution of intensities with theoretical distribution curves for the centric (I), acentric (II) and hypercentric (III) cases. hkl data: circles; $hk0$ data: triangles.

Powder patterns of Pb_3UO_6 were also recorded with a Philips PW1051 counter diffractometer at a scanning speed of $\frac{1}{4}^\circ$ per minute, with Cu $K\alpha$ radiation. In order to minimize possible preferred orientation, the specimen powder, prepared by prolonged grinding of the polycrystalline Pb_3UO_6 , was sieved through a 400 mesh screen and exposed in a rotating sample holder, the thickness of the specimen being approximately 0.5 mm. Intensities of powder reflexions recorded from several samples were found to differ by no more than 3%. The intensities of non-overlapping reflexions were estimated from peak areas and the derived F_o values used in the later stages of the analysis to check the single-crystal data and to assess qualitatively the influence of absorption and extinction effects.

Examination of the full set of data revealed the following systematic absences: $h0l$ with h odd and $0kl$ with $k+l$ odd, indicating as possible space groups $Pna2_1$ (no. 33) and $Pnam$ (non-standard $a\bar{c}b$ setting of no. 62). A statistical analysis of the three-dimensional data, using the $N(z)$ test of Howells, Phillips & Rogers (1950), gave a distribution coinciding almost exactly with the theoretical curve for 'hypercentric symmetry' (Fig. 1), indicating an atomic arrangement of higher symmetry than required by the space group (Lipson & Woolfson, 1952). Although not conclusive, this test seemed to favour the centrosymmetric space group, which was therefore chosen to initiate the analysis, and later results did not contradict this choice.

Location of metal atoms

The structure analysis was initiated with a three-dimensional Patterson distribution, calculated on an IBM 7044 computer at Melbourne University, using Dr J. C. B. White's Fourier program MU-FRI. Because of the presence of 32 heavy atoms in the unit cell, with nearly equal scattering powers, it was naturally not possible to isolate and identify individual U-U, Pb-Pb and U-Pb vectors. Approximate positions of the metal atoms could be deduced only by determining regions of possible atom concentrations from a careful examination of the peak distribution on all Harker lines and sections of the space group, and their correlation with interaction vector peaks in the general distribution.

All significant peaks in the three-dimensional vector distribution are concentrated in, or very near, sections $P(u, v, 0)$, $P(u, v, \frac{1}{4})$ and $P(u, v, \frac{1}{2})$ (Fig. 2) and within these sections near lines $v = 0, \frac{1}{4}, \frac{1}{2}$, indicating that the metal atoms are situated on or near planes perpendicular to the b and c axes, spaced $\frac{1}{4}b$ and $\frac{1}{4}c$ respectively apart, with a more general distribution along a . From the distribution on Harker lines $P(\frac{1}{2}, v, 0)$ and $P(0, 0, w)$, these planes could be placed at $y \sim 0, \frac{1}{2}$ and $\frac{1}{4}, \frac{3}{4}$ and at $z \sim 0, \frac{1}{2}$. To explain the vector peaks at $w \sim \frac{1}{4}$, atoms must be assumed also on levels $z = \frac{1}{4}, \frac{3}{4}$, in special positions on the mirror planes. This concentration of the metal atoms near the intersection lines of the two sets of planes was also confirmed quite convincingly by the

Harker section $P(\frac{1}{2}, v, w)$, which shows dense areas only near the corners, at $u, w = 0, 0; 0, \frac{1}{2}, 0; \frac{1}{2}, \frac{1}{2}$. All Harker peaks must therefore lie near the zero and half-axis lines of the three Harker sections. By examination of the shapes and positions of the peaks and by correlation with other sections, the deviations of corresponding atoms from the intersection lines and also their approximate x coordinates could be deduced. In this way, it was possible to place the 32 metal atoms of the unit cell in two eightfold general positions and four fourfold special positions on the mirror planes.

Comparison of all possible calculated metal atom interaction vectors with the observed three-dimensional vector distribution showed reasonable agreement, no vector end points falling on negative or low density areas, and all higher peaks being accounted for. The calculated vector end points are marked as crosses in the sections of Fig. 2, although in some cases the end points are slightly above or below the section plane, usually in areas of higher density.

The derived coordinates of the six metal atoms in one cell octant ($a/2, b, c/4$) are given in Table 1 and a diagram of the metal atom positions in the whole cell in Fig. 3.

Table 1. Fractional coordinates of metal atoms derived from the Patterson distribution

Atom	Number of positions	x	y	z
1	4(c)	0.033	0.017	0.250
2	4(c)	0	0.508	0.250
3	4(c)	0.350	0.736	0.250
4	4(c)	0.183	0.264	0.250
5	8(d)	0.267	0.008	0.033
6	8(d)	0.417	0.264	0

Differentiation of U and Pb atoms and location of oxygen atoms

The identification of the U, Pb and O atoms was attempted by conventional Fourier synthesis, although it was to be expected that the analysis would not be straightforward because of the small difference in scattering powers of U and Pb, the very small contribution of the O atoms and the uncertainty in the scattering curves of the metal atoms, especially uranium. In previous structure analyses of uranates and other compounds of six-valent uranium, structure factors based on U^0 (e.g. Roof, Cromer & Larson, 1964) as well as on U^{6+} (Allpress, 1965) have been used, and the published values of the anomalous dispersion corrections for uranium vary over a wide range (Dauben & Templeton, 1955; Roof, 1961).

The F contributions of the metal atoms derived from the Patterson distribution were initially calculated with the use of an 'average' scattering curve [$f(\text{U}^{6+}) + 3f(\text{Pb}^{2+})$]/4 based on the form factors listed in *International Tables for X-ray Crystallography* (1962), with $f(\text{Pb}^{2+})$ extrapolated from $f(\text{Pb}^{3+})$ and $f(\text{Pb}^0)$. Corrections for anomalous dispersion were not applied and,

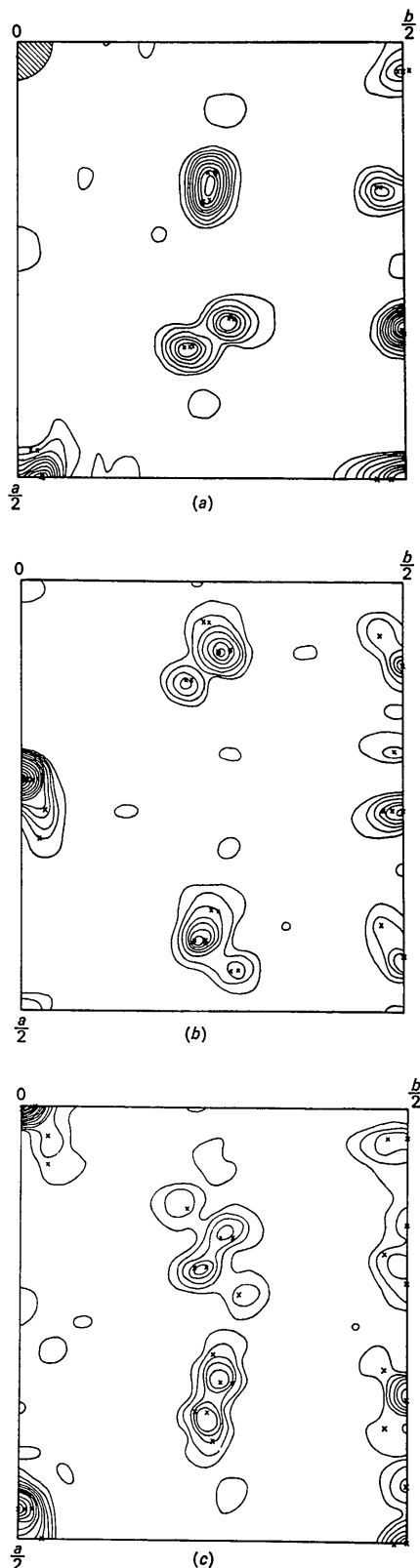


Fig. 2. Sections through the three-dimensional Patterson distribution. (a) $P(u, v, 0)$, (b) $P(u, v, \frac{1}{4})$, (c) $P(u, v, \frac{1}{2})$.

with $B=0$, this set of structure factors gave an agreement of $R=0.38$.

The first Fourier synthesis, using for the calculation F_o terms with the signs of the metal atom structure factors and omitting terms with $F_c < F_o/3$, showed small shifts in the metal atom positions, all peak heights being approximately equal, but, owing to pronounced series termination ripples, gave no indication of the oxygen positions. A difference synthesis with recalculated F_c values for the metal atoms ($R=0.33$) was therefore carried out simultaneously with a second ρ_o synthesis. The $\Delta\rho$ distribution gave negative peaks in the metal positions, indicating either an incorrect scat-

tering curve or the influence of appreciable extinction errors in the strong low-angle F_o terms. However, in the eightfold position of atom 6 (Table 1), the negative excursion was much less than in the other positions ($-30 \text{ e.}\text{\AA}^{-3}$ compared with *ca.* $-70 \text{ e.}\text{\AA}^{-3}$). The peak heights in the ρ_o distribution did not vary appreciably (all *ca.* $300 \text{ e.}\text{\AA}^{-3}$, but electron counts of peak volumes gave 89 e for position 6 and 77–81 e for the other peaks. Furthermore, the $\Delta\rho$ distribution revealed some distinct small peaks of height 15–20 $\text{e.}\text{\AA}^{-3}$ in the vicinity of position 6, which could be correlated with less distinct positive regions in the ρ_o distribution. Four of these peaks were in general positions and two in special positions, surrounding atom 6 octahedrally at distances of 1.9–2.2 \AA . This corroborative evidence seemed to indicate definitively that position 6 is occupied by uranium, which is coordinated to six oxygen atoms at the corners of an octahedron. Thus, 40 oxygen atoms out of 48 in the unit cell could be accounted for. Two further small peaks, situated in special positions on the mirror planes and not forming part of the octahedra, could be identified in both distributions and were assumed as the remaining oxygen atoms, completing the provisional placement of all atoms in the unit cell.

Structure factors based on coordinates of all atoms were calculated with individual scattering factors of U^{6+} , Pb^{2+} and O^{2-} , using Suzuki's (1960) values for the latter, and with an overall temperature factor, $B=0.5$, deduced from a provisional $\ln(F_c(\text{metal})/F_o)$ versus $\sin^2\theta$ plot. The resulting R value was 0.21, the drop by 12% indicating that the analysis was proceeding in the right direction and that the structure was probably sufficiently defined for least-squares refinement.

Refinement

Least-squares calculations were carried out on an IBM 1620 computer with Dr G.A. Mair's block-diagonal approximation program SFLS, which minimizes $\sum w(|F_o| - |F_c|)^2$. Weighting schemes of Mills & Rollett (1961) were used, initially as $\sqrt{w}=1$ for $k|F_o| \leq F^*$ and $\sqrt{w}=F^*/k|F_o|$ for $k|F_o| > F^*$, with $F^*=600$ (the highest values of F_o being about 1500) and in the final stages as $\sqrt{w}=1/[1+(k|F_o|-b)^2/a^2]^{1/2}$ with $a=560$ and $b=350$.

The first least-squares cycle was calculated with scattering factors of U^{6+} , Pb^{2+} and O^{2-} , the f values of the metals being adjusted for anomalous dispersion, using Dauben & Templeton's (1955) values of $\Delta f'$ and $\Delta f''$. Positional parameters and individual isotropic temperature factors of only the metal atoms were varied, with an initial value of $B=0.5$ for all atoms. The agreement improved to $R=0.137$; the shifts of the metal atoms did not exceed 0.02 \AA and the resulting values of B_{Pb} were reasonable, varying from 0.30 to 0.44. However, the temperature factor for uranium was negative ($B_{\text{U}}=-0.18$), a situation which has also been encountered in structure analyses of other uranium compounds (*cf.* Cromer, Larson & Roof, 1964). In the present case, the cause of the anomaly could be either

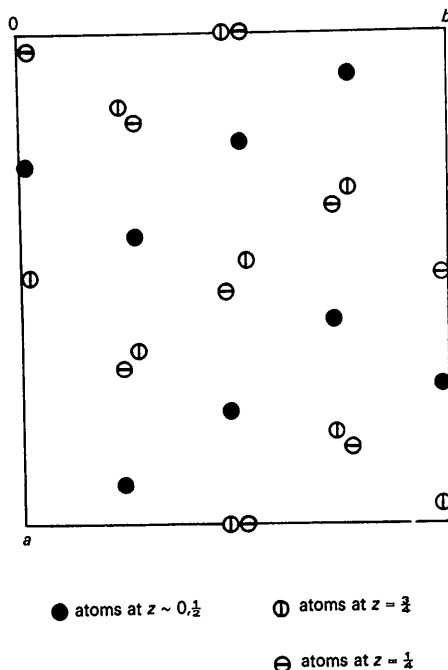


Fig. 3. Positions of metal atoms deduced from the Patterson distribution.

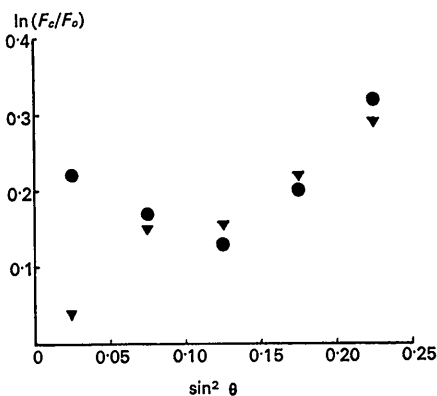


Fig. 4. Plots of $\ln(F_c/F_o)$ against $\sin^2\theta$ for classes of reflexions with $l=2n$ (circles) and $l=2n+1$ (triangles), the former indicating influence of extinction and/or absorption on low order reflexions. (F_c and F_o represent the mean values in five ranges of $\sin^2\theta$.)

an incorrect scattering curve for uranium or absorption and/or extinction errors in the strong low-angle terms. That the latter are not negligible can be seen from a comparison of separate plots of $\ln(F_c/F_o)$ versus $\sin^2\theta$ for layers with $l=2n$, which contain all the strong low-angle reflexions, and those with $l=2n+1$ (Fig. 4). Whilst the second plot is normal and corresponds to $B \sim 0.5$, the first shows a marked decrease at low angles, simulating a negative temperature factor.

To test the effect of variation in the uranium scattering curve, the next two least-squares cycles were calculated with scattering factors of neutral atoms. The values of $f(U^0)$, $f(Pb^0)$ and $f(O^0)$ were those given in *International Tables for X-ray Crystallography* (1962), with the metal f curves adjusted for anomalous dispersion. All positional and individual isotropic thermal parameters were varied, with input values of $B_U = 0.5$, $B_{Pb} = 0.5$, $B_O = 1.0$. The agreement improved to $R = 0.096$, with metal atom shifts all less than 0.003 \AA and oxygen shifts up to 0.06 \AA , but the uranium temperature factor was still negative ($B_U = -0.12$).

In order to reduce the influence of extinction and possible absorption errors, 29 low-angle terms with large values of $F_c - F_o$ were omitted from subsequent cycles. This resulted in an initial decrease of R to 0.078 , no negative temperature factors were encountered and the refinement converged quite satisfactorily to $R = 0.068$. In the last cycle, the shifts in positional parameters were less than 0.001 \AA for the metal atoms, less than 0.005 \AA for the oxygen atoms and the changes in thermal parameters were less than 0.05 . The final value of B_U was 0.12 , average $B_{Pb} \sim 0.62$ ($0.50-0.75$) and average $B_O \sim 0.9$ ($0.4-1.5$).

As an independent check, F_o values of non-overlapping powder reflexions were evaluated from slow-scan

diffractometer traces. Since extinction is negligible for a polycrystalline powder and absorption in a flat powder specimen is independent of θ (Klug & Alexander, 1954), the F_o values for strong low-angle powder reflexions could be expected to show better agreement with calculated structure factors than those evaluated

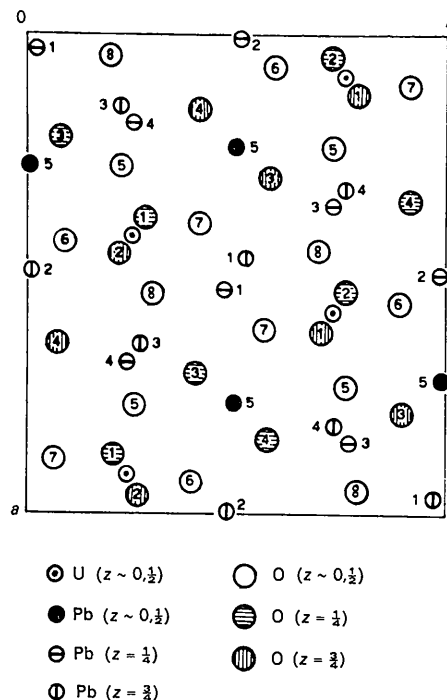


Fig. 5. Final atomic positions in the unit cell of Pb_3UO_6 .

Table 2. Comparison of structure factors from powder and single-crystal data

hkl	$\sin \theta/\lambda$	F_c	KF_o (powder)	F_o (single crystal)
111	0.0812	169	140	200
210	0.0828	103	90	150
211	0.1022	99	90	110
121	0.1072	106	95	110
221	0.1244	155	150	170
130	0.1263	260	240	260
131	0.1403	307	300	310
212	0.1470	1026	1010	840
410	0.1508	879	850	800
231	0.1537	139	140	150
040	0.1614	2079	2120	1490
222	0.1630	1438	1400	1070
420	0.1662	1413	1360	1130
312	0.1683	209	230	240
232	0.1862	733	800	670
430	0.1893	809	870	710
601	0.2265	588	610	570

$$F_o(\text{powder}) = \left[\frac{I}{p} \cdot \frac{\sin^2 \theta \cos \theta}{1 + \cos^2 2\theta} \right]^{\dagger}$$

I = peak area

p = multiplicity of powder reflexions

$K = \Sigma F_c / \Sigma F_o$ (powder).

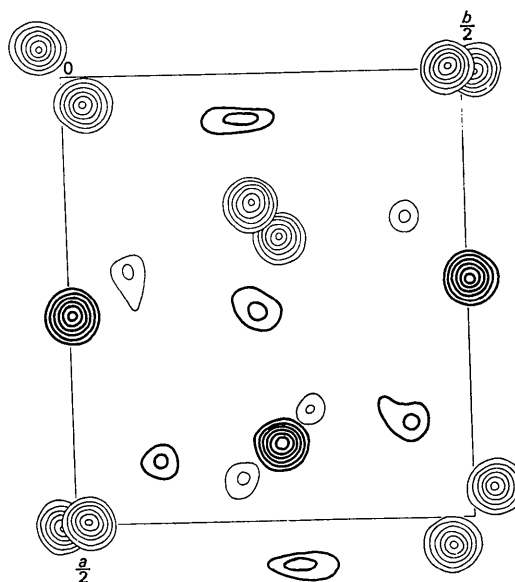


Fig. 6. Superimposed sections of the three-dimensional electron density distribution, taken through atomic centres parallel to (001). Contours are at intervals of 50 e. \AA^{-3} for the metal atoms and 10 e. \AA^{-3} for oxygen atoms; overlapping pairs of atoms are indicated by heavier contour lines.

from single-crystal data. This was proved quite convincingly by the values listed in Table 2, the R value for the 17 powder reflexions which could be measured accurately being 0.042, compared with $R=0.20$ for the same terms of the single-crystal data.

Re-inclusion of the 29 omitted terms, corrected empirically from the powder data, did not impair the agreement; indeed, a slightly better overall value of $R=0.067$ was obtained in the final calculation of structure factors. (With unobserved terms included, taking F_o at half the minimum observable value, $R=0.106$.)

In view of the reasonably good agreement of F_o and F_c values and the very small shifts in the last least-squares calculations, the atomic positions, especially of the metal atoms, were regarded as sufficiently certain to define the essential features of the structure of Pb_3UO_6 , which was the main purpose of the investigation.

Fig. 5 shows the distribution of atoms in the unit cell viewed down the c axis, and a composite electron density map of a quarter-cell is reproduced in Fig. 6. The final atomic coordinates and their mean standard deviations are listed in Table 3, the corresponding interatomic distances in Table 4, and values of F_o and F_c in Table 5.

Table 3. Atomic parameters as fractions of unit-cell parameters

Atom	Number of positions	x	y	z
U	8(d)	0.414	0.260	0.002
Pb(1)	4(c)	0.032	0.026	0.250
Pb(2)	4(c)	0.004	0.515	0.250
Pb(3)	4(c)	0.353	0.729	0.250
Pb(4)	4(c)	0.183	0.263	0.250
Pb(5)	8(d)	0.269	0.003	0.031
O(1)	4(c)	0.373	0.291	0.250
O(2)	4(c)	0.041	0.731	0.250
O(3)	4(c)	0.208	0.089	0.250
O(4)	4(c)	0.348	0.916	0.250
O(5)	8(d)	0.232	0.735	0.032
O(6)	8(d)	0.433	0.098	0.043
O(7)	8(d)	0.112	0.920	0.043
O(8)	8(d)	0.045	0.206	0.054

$\sigma(x)_U=0.004 \text{ \AA}$; $\sigma(x)_{Pb}=0.004 \text{ \AA}$; $\sigma(x)_O=0.09 \text{ \AA}$
 [Calculated according to Cruickshank's (1960) formula.]

Table 4. Shortest interatomic distances

(Possible error $\pm 0.1 \text{ \AA}$)			
U-O(1)	2.15 \AA	Pb(2)-O(6')	2.76 \AA
U-O(2)	2.19	Pb(3)-O(4)	2.31
U-O(5)	2.03	Pb(3)-O(5)	2.45
U-O(6)	2.05	Pb(3)-O(2)	2.62
U-O(7)	2.04	Pb(3)-O(8)	2.88
U-O(8)	1.90	Pb(4)-O(3)	2.18
Pb(1)-O(7)	2.41	Pb(4)-O(8)	2.57
Pb(1)-O(3)	2.53	Pb(4)-O(5)	2.62
Pb(1)-O(8)	2.75	Pb(4)-O(1)	2.64
Pb(1)-O(1)	3.14	Pb(5)-O(3)	2.24
Pb(1)-O(7)'	3.18	Pb(5)-O(4)	2.36
Pb(1)-O(8)'	3.90	Pb(5)-O(7)	2.38
Pb(2)-O(4)	2.30	Pb(5)-O(6)	2.54
Pb(2)-O(6)	2.40	Pb(5)-O(5)	2.91
Pb(2)-O(2)	2.72	Pb(5)-O(5)'	3.35

Description and discussion of the structure

The uranium atoms on planes $z \sim 0$ and $z \sim \frac{1}{2}$ are surrounded in a nearly regular square array by four oxygen atoms O(5), O(6), O(7) and O(8), two below and two above the planes $z=0$ or $z=\frac{1}{2}$, and by oxygen atoms O(1) and O(2) on planes $z=\frac{1}{4}$ and $z=\frac{3}{4}$. These six oxygen atoms thus form a somewhat distorted octahedron around the uranium, with the apex oxygen atoms O(1) and O(2) at a slightly greater distance from the central uranium than the other four. The diagonal between the apices is tilted out of the z direction by about 18° in a direction nearly parallel to the diagonals of the ab plane and is approximately normal to the plane defined by the other four oxygens. The apex oxygen atoms are shared by two octahedra with opposite tilts, resulting in puckered chains of composition $(UO_3)_\infty$ along the c axis. The occurrence of UO_3 chains in Pb_3UO_6 means that only five of the six oxygen atoms in the formula unit (40 in the unit cell) are included in the coordination polyhedra of uranium. The remaining eight oxygen atoms in the unit cell are distributed between the lead atoms, well outside the coordination range of uranium. A projection of the disposition of atoms down the c axis, with outlines of the octahedra dotted and Pb-O distances of less than 3 \AA indicated by full lines, is reproduced in Fig. 7.

Lead atoms at $z=\frac{1}{4}$ and $z=\frac{3}{4}$, situated between the chains of octahedra are coordinated primarily to four oxygen atoms at the corners of four separate octahedra from two neighbouring chains. However, owing to the different disposition and tilt of these octahedra, the oxygen environment is different for each of the four lead atoms Pb(1-4). Pb(2) is situated between two chains of octahedra with corners opposing across the screw axis at $x=0, y=\frac{1}{2}$ and, because of the tilt of the octahedra, the four corner oxygen atoms O(6) do not form a square but a 'trapezoidal' array, with the lead atom nearer to the longer side. The tilt also brings O(2) into the coordination range of Pb(2), resulting in a nearly regular pentagonal arrangement, with O(4) completing a distorted pentagonal pyramid. The disposition of oxygen around Pb(3) and Pb(4) is similar, the lead atoms again being coordinated to corner oxygen atoms O(5) and O(8) of four octahedra, with O(1) and O(3) or O(2) and O(4) completing the pentagonal pyramids. Atoms Pb(1) are situated between two chains of octahedra with edges opposing across the screw axes at $x=0, y=0$, and $x=\frac{1}{2}, y=\frac{1}{2}$ and having tilts in the same direction. The two pairs of oxygen atoms O(7) and O(8) from the two chains form a nearly rectangular array on one side of the respective Pb(1) atom, drawing it away from the screw axis, and O(3) on the same z level completes an irregular fivefold coordination unit. The five Pb-O distances are between 2.4 and 2.8 \AA (Table 4), but there are three additional oxygen atoms, O(1) and two O(7), at distances 3.1 and 3.2 \AA . If these are regarded as still coordinated to Pb(1), the result is an irregular eightfold coordination, with the five nearer

oxygen atoms all on one side of the lead atom and the remaining three on the other.

The remaining eight lead atoms Pb(5) lie in channels between four chains of octahedra at approximately the same z level as the nearest oxygen atoms in the octahedra, O(6) and O(7), which together with O(3) and O(4) form a rather odd double fourfold coordination unit, O(3) and O(4) being shared between two lead atoms.

The structure derived for Pb_3UO_6 is thus rather irregular, especially in regard to the oxygen environment of lead and the distribution of oxygen atoms outside the UO_5 chains. There is little structural information about the oxygen coordination of lead in more complex ternary compounds, but some of the published work, notably the structure analysis of linarite, $\text{PbCuSO}_4(\text{OH})_2$, by Bachmann & Zemmann (1961), also indicates an unusual oxygen environment (three- to eight-fold) of lead(II).

The U–O and Pb–O distances listed in Table 4, although probably reliable to only ± 0.1 Å, owing to possible errors in the oxygen positions, are within the accepted limits cited in the literature.

Uranium(VI)–oxygen distances from 1.8 to 2.3 Å, depending on the number and nature of the other bonds formed by the oxygen atom, have been reported for uranate structures.

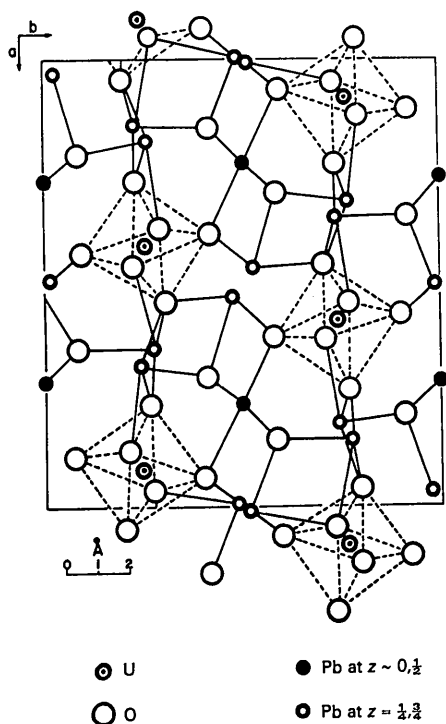


Fig. 7. c -Axis projection of the structure, showing the disposition of chains of uranium–oxygen octahedra (viewed down the chain direction). Full lines indicate the shortest Pb–O approach distances (< 3 Å).

In Pb_3UO_6 , the distances U–O(1) and U–O(2) appear to be significantly longer than the other four, which is to be expected, since these oxygen atoms are shared between two uranium atoms. The U–O distances of the four ‘unshared’ oxygens are, on the other hand, somewhat longer than the accepted uranyl bond length (*ca.* 1.8 Å); this is also understandable, since there are four such oxygen atoms compared with two in the linear uranyl group O–U–O.

The short U–O(8) distance of 1.90 Å, which causes an irregular distortion of the octahedra, may be the result of an error in the position of O(8). However, it is interesting to note that, whereas the shortest approach distances of O(5), O(6) and O(7) to lead atoms are of the order of 2.4 Å, O(8) has its nearest lead neighbour at *ca.* 2.6 Å. As a consequence of this, one could probably expect a stronger and hence shorter bond between O(8) and uranium. A detailed balancing of U–O bond lengths and bond strengths as proposed by Zachariassen (1954) was not possible since all oxygen atoms in the UO_6 octahedra are also bonded to some lead atoms, at widely varying distances.

Judging from the results of the analysis, there seems to be little doubt about the correctness of the metal atom positions and also about the octahedral oxygen environment of uranium, but the positions of the remaining oxygen atoms O(3) and O(4) are less certain. Thus, the rather short distance Pb(4)–O(3) of 2.18 Å is probably due to an error in the oxygen parameter, although similar lead(II)–oxygen distances have been found for one of the bivalent lead ions in Pb_3O_4 (2.15 Å) by Byström & Westgren (1943) and for yellow PbO (2.21 Å) independently by Kay (1961) and by Leciejewicz (1961) from neutron diffraction data.

The structure of Pb_3UO_6 differs radically from those of the other known uranates M_3UO_6 ($\text{M} = \text{Ca}, \text{Sr}, \text{Ba}, \text{Cd}$), all of which contain isolated UO_6 octahedra, with the M atoms in more or less symmetrical twelve- and six-fold coordination to oxygen. Because of the layer structure of PbO and the known asymmetric disposition of oxygen around lead in PbO and a number of other compounds, the symmetrical cryolite type structure is probably less favourable for Pb_3UO_6 than for uranates of the alkaline earths and cadmium, the oxides of which have sodium chloride structures with the required symmetrical sixfold coordination.

A more detailed investigation of the structure would require data reliably corrected for absorption and extinction, as well as a better knowledge of the true scattering curves of the metal atoms.

The writer is indebted to Dr A. McL. Mathieson and Dr A. D. Wadsley for helpful discussions and for permission to use some of their experimental facilities, to Mr J. Fridrichsons for a great deal of valuable advice, to Dr B. R. Penfold for making available a number of IBM 1620 programs, and to Dr J. C. B. White for the use of his IBM 7044 programs and for help and advice concerning the computational work.

References

- ALLPRESS, J. G. (1965). *J. Inorg. Nucl. Chem.* **27**, 1521.
 BACHMANN, H. G. & ZEMANN, J. (1961). *Acta Cryst.* **14**, 474.
 BYSTRÖM, A. & WESTGREN, A. (1943). *Ark. Kemi Min. Geol.* **16B**, no. 14.
 CROMER, D. T., LARSON, A. C. & ROOF, R. B. (1964). *Acta Cryst.* **17**, 272.
 CRUICKSHANK, D. W. J. (1960). *Acta Cryst.* **13**, 774.
 DAUBEN, C. H. & TEMPLETON, D. H. (1955). *Acta Cryst.* **8**, 841.
 FRONDEL, C. & BARNES, I. (1958). *Acta Cryst.* **11**, 562.
 HOWELLS, E. R., PHILLIPS, D. C. & ROGERS, D. (1950). *Acta Cryst.* **3**, 210.
International Tables for X-ray Crystallography (1962). Vol. III, pp. 202, 206, 212. Birmingham: Kynoch Press.
 KAY, M. I. (1961). *Acta Cryst.* **14**, 80.
 KLUG, H. P. & ALEXANDER, L. E. (1954). *X-ray Diffraction Procedures*, p. 376. New York: John Wiley.
 KOVBA, L. M., POLUNINA, G. P., SIMANOV, YU. P. & IPOLITOVA, B. A. (1961). *Issledovania v Oblasti Khimii Urana*, p. 15. Moscow Univ. Press.
 LECIEJEWICZ, J. (1961). *Acta Cryst.* **14**, 66.
 LIPSON, H. & WOOLFSON, M. M. (1952). *Acta Cryst.* **5**, 680.
 MILLS, O. S. & ROLLETT, J. S. (1961). *Computing Methods and the Phase Problem in X-ray Crystal Analysis*, p. 117. Oxford: Pergamon Press.
 RIETVELD, H. M. (1966). *Acta Cryst.* **20**, 508.
 ROOF, R. B. (1961). *Acta Cryst.* **14**, 934.
 ROOF, R. B., CROMER, D. T. & LARSON, A. C. (1964). *Acta Cryst.* **17**, 701.
 RÜDORFF, W. & PFITZER, F. (1954). *Z. Naturforsch.* **9b**, 568.
 SAMSON, S. & SILLÉN, L. G. (1947). *Ark. Kemi Min. Geol.* **25A**, no. 21.
 SLEIGHT, A. W. & WARD, R. (1962). *Inorg. Chem.* **1**, 790.
 ZACHARIASEN, W. H. (1954). *Acta Cryst.* **7**, 795.

Acta Cryst. (1967). **23**, 272

The Crystal and Molecular Structure of *meso*-3,3'-Di-(*p*-bromophenyl)bi-3-phthalidyl

BY V. KALYANI, H. MANOHAR* AND N. V. MANI†

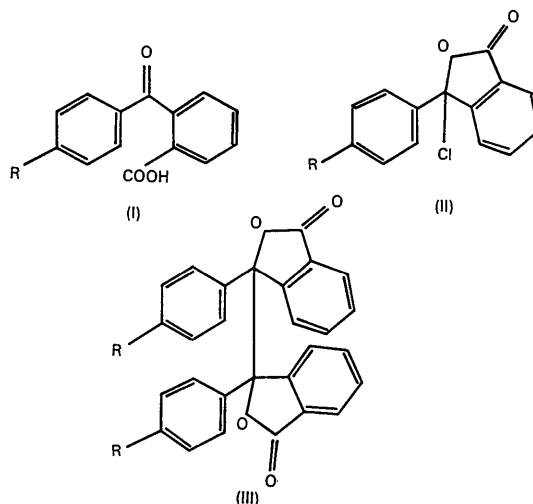
Department of Physics, Indian Institute of Science, Bangalore 12, India

(Received 26 October 1966)

The crystal structure of the title compound has been determined by the heavy-atom method and Fourier techniques using visually estimated photographic data. It crystallizes in the space group $P\bar{1}$ with cell dimensions $a=7.98$, $b=8.08$, $c=9.66$ Å, $\alpha=85^\circ 23'$, $\beta=98^\circ 24'$ and $\gamma=104^\circ 41'$. The parameters have been refined by three-dimensional least-squares procedures with anisotropic thermal vibrations for all the atoms. The final R index for 932 observed reflexions is 0.096. It has been established that the stereoisomer taken up for investigation is the *meso* form existing in a staggered configuration. Two characteristics of the lactone group, *viz.*, the inequality of the C–O bonds and the planarity of the group are also confirmed in the present study.

Introduction

A variety of reducing agents convert *o*-benzoylbenzoic acids (I) and their acid chlorides (II) to 3,3'-diarylbi-phthalidyls (III). Two isomers, *viz.* the racemic (DL) [IV and V, one being the *dextro* (D) and the other the *laevo* (L) form] and the *meso* form (VI) having structure (III) are theoretically possible. However, no attempt has so far been made to define their stereochemistry. This information would be of considerable value in understanding the steric factors involved in their formation, particularly because the two stereoisomers are formed in unequal proportions. In view of this, the more



* Present address: Department of Inorganic and Physical Chemistry, Indian Institute of Science, Bangalore 12, India.

† Present address: Laboratorium voor Structuurchemie, Rijksuniversiteit Groningen, Bloemsingel 10, Groningen, The Netherlands.